

PLANETARY NEBULAE

M J Barlow

Dept. of Physics & Astronomy
University College London
Gower St., London WC1E 6BT

ABSTRACT

A large number of infrared fine structure lines have now been observed from planetary nebulae and they provide a powerful tool for the determination of nebular physical parameters and abundances, for both ionised and neutral regions. H_2 line emission has been detected from 50% of the PN so far surveyed and, rather surprisingly, shows a higher probability of being detected around old, low-density nebulae than around young, dense nebulae. Photodissociation zone models seem promising in some cases. Spectroscopy at $10\mu\text{m}$ shows that of the nebulae with detectable continua, 33% show silicate features, 25% show SiC features and 42% show strong UIR bands. These feature types follow a sequence of increasing nebular C/O ratio. A number of carbon-rich PN have also been found to exhibit a very strong $30\mu\text{m}$ feature which has been attributed to MgS. Recent work on the modelling of the dust emission continua and on the derivation of gas-to-dust mass ratios is also reviewed.

Keywords: Fine Structure Lines, Molecular Hydrogen, Dust Emission Features, Dust Continua

1. INTRODUCTION

In this review I will concentrate on the developments that have occurred in the field of infrared spectroscopy of planetary nebulae (PN) since 1983. Work prior to that date was covered in a number of reviews given at IAU Symposium No. 103. In addition, reviews addressed to the dust emission properties of PN were given by Preite-Martinez (Ref. 61) and Roche (Ref. 63) at IAU Symposium No. 131.

I have divided the review into four parts. Section 2 discusses ionic fine structure line emission from PN. Section 3 covers the observations and interpretation of molecular hydrogen line emission from planetary nebulae. Section 4 reviews the work on the identified and unidentified dust emission features seen in the IR spectra of PN, while Section 5 discusses the overall energetics of the continuum

dust emission observed from PN and the dust-to-gas mass ratios that are derived for these objects.

2. FINE STRUCTURE LINES

More than twenty different infrared fine structure lines have now been observed from planetary nebulae, making these objects by far the richest sources of such lines. Work up to the end of 1982, reviewed by Dinerstein (Ref. 23), had led to ground-based detections of four infrared fine structure lines, while *KAO* observations has added another eight lines. Since then, a further three lines have been found by means of ground-based observations, five through *KAO* observations, and three neon fine structure lines were found in the spectra of PN by the *IRAS* LRS survey. Table 1 lists the lines found since 1983 and gives the appropriate references.

The low excitation energies of infrared fine structure transitions ensure that their strengths are insensitive to electron temperature, unlike optical or UV forbidden lines. Although ionic abundances can therefore be derived without knowledge of the electron temperature, it is necessary to know the electron density when analysing the IR fine structure lines. This is because at typical PN electron densities collisional de-excitation can often compete significantly with radiative de-excitation. The *critical density*, $n_e(\text{crit})$, of a transition is defined as the electron density at which the rate of collisional excitation and de-excitation out of the upper level of the transition is equal to the downward radiative de-excitation rate. For electron densities much smaller than $n_e(\text{crit})$, collisional excitations from the ground state to the upper level (proportional to $n_e n_i$) are balanced by radiative de-excitations and so the line flux is proportional to $n_e n_i dV$, where dV is the emitting volume. For electron densities much larger than $n_e(\text{crit})$, collisional excitation and de-excitation dominate, a Boltzmann equilibrium of level populations is established, and so the line flux is proportional to $n_i dV$, the total number of ions.

Ions with p^1 and p^5 structure (*e.g.* C II and Ne II) have doublet ground state fine structure splitting, and so only one fine structure transition results. However, p^2

Table 1. IR fine structure lines discovered in PN spectra since 1983

ION	λ (μm)	Ref.
Si VI	1.96	4
Si VII	2.48	4
Ni II	6.64	14
Ne VI	7.65	60
Cl IV	11.77	64
Ne V	14.33	60
Ne III	15.56	60
Ne III	36.02	68
N III	57.30	27,32
O I	145.5	28
C II	157.7	28

Table 2. Critical densities for some infrared fine structure lines

ION	λ (μm)	n_e (crit) (cm^{-3})
N II	121.7	25
	203.9	250
O III	51.82	600
	88.36	5000
S III	33.47	4000
	18.71	4×10^4
Ne III	36.02	3×10^4
	15.56	4×10^5
Ar III	21.83	4×10^4
	8.99	4×10^5
Ne V	24.28	1×10^5
	14.33	4×10^5

and p^4 ions (e.g. O III and O I) have triplet fine structure splitting of their ground states, giving rise to two fine structure transitions. The different transition probability and collision strength for each line means that each will have a different critical density and so at electron densities lying between these two values, the flux of the line with the higher critical density will be proportional to $n_e n_i$, while the flux of the line with the lower critical density will only be proportional to n_i . The ratio of the two line strengths can therefore be used to derive the nebular electron density. Table 2 presents the critical densities (calculated for $T_e = 10^4\text{K}$) for the IR fine structure lines for a range of p^2 and p^4 ions commonly found in planetary nebulae. It can be seen that suitable IR fine structure line pairs are available for the derivation of densities over the whole density range normally encountered amongst PN (and H II regions). The two spectrometers on board *ISO* will therefore be able to carry out rapid and accurate abundance surveys for a wide range of objects.

The ratio of the strength of an IR fine structure line to that of a collisionally excited optical or UV line from the same ion is a good diagnostic of electron temperature, although care has to be exercised to properly correct for the effects of differential extinction. For a number of PN, Dinerstein *et al.* (Ref. 26) have compared the electron temperatures derived from [O III] 4363/5007Å and 52μm/5007Å ratios and have found the former to be systematically higher. Since λ4363 requires the highest excitation energy, it would be enhanced preferentially in regions of higher than normal temperature within a nebula. Dinerstein *et al.* invoked such temperature fluctuations to explain the higher temperatures derived using λ4363 and noted that, if indeed present, the oxygen abundances traditionally derived using 4363/5007Å temperatures would be too low by about 0.2 dex, sufficient to account for a long-standing discrepancy between the solar oxygen abundance and those of PN. However, it should be noted that Lambert *et al.* (Ref. 46) have found that the distribution of oxygen abundances derived for M and C type stars are similar to those found for PN, so that the Sun may really have a higher than average oxygen abundance.

Shure *et al.* (Ref. 67) used the O IV 25.9μm/1400Å intensity ratio observed for NGC 7662 to derive an electron temperature for the O IV emitting zone that was in good agreement with ionisation structure model predictions for this nebula (Ref. 36). Unfortunately, the situation for Ne V has been more uncertain. Pottasch *et al.* (Ref. 60) compared the *IRAS* LRS 14.3μm [Ne V] fluxes for a number of PN with those published for [Ne V] 3426Å and, using the [Ne V] collision strengths of Aggarwal (Ref. 1) and [Ne III] 15.6μm/3868Å electron temperatures, obtained electron densities much higher than determined by other methods. Clegg *et al.* (Ref. 19) found that for

NGC 3918 the use of Aggarwal's collision strengths predicted a [Ne V] 14.3μm line flux much larger than measured by *IRAS*, when normalised to the observed 3426Å relative line flux from slit spectra. Recently, however, Rowlands *et al.* (Ref. 66) have compared large-beam flux measurements obtained at both 3426Å and 24.3μm for a dozen PN, and have derived very plausible electron temperatures for the Ne V zones, using Aggarwal's collision strengths. The earlier problems may therefore have been due to narrow-slit 3426Å spectra giving overestimates for the integrated strengths from the entire nebulae.

The *IRAS* mission led to the unexpected detection of [Ne VI] 7.65μm in the LRS spectrum of NGC 6302 (Ref. 60). To produce this ion from Ne V requires an ionisation potential of 126eV, indicating a very high effective temperature for the central star. Ashley & Hyland (Ref. 4) subsequently detected [Si VI] 1.96μm and [Si VII] 2.48μm from this nebula, ions which respectively require 167eV and 205eV for their production. They estimated an effective temperature of 430,000K for the central star. A very large range of ionisation states therefore exist in this and in a few similar PN, and the ionisation correction factors previously used to derive abundances from their optical and UV spectra are likely to have been significantly in error, as pointed out by Roche & Aitken (Ref. 65).

Recommended transition probabilities and electron collision strengths for fine structure lines (as of 1982) were tabulated by Mendoza (Ref. 50). Since then, new collision strength calculations have been carried out for a number of ions. These include C II (Refs. 38, 48, 44), N III and Ne VI (Ref. 17), O IV (Ref. 37), Ne II (Ref. 7), Ne III (Ref. 16), Mg IV and Mg V (Ref. 51), Al V, Si VI and Si VII (Ref. 15), S IV (Ref. 43) and Ar VI (Ref. 79).

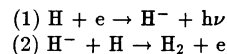
Finally, in addition to observations of fine structure lines from the ionised zones of PN, it has been possible to observe the fine structure lines of [O I] 63μm and 146μm and [C II] 158μm from the neutral zones around some PN. Watson (Ref. 76) has shown how these three lines may be used to derive neutral region densities and temperatures (if a C/O ratio is assumed). [O I] 63μm was first detected from NGC 7027 by Melnick *et al.* (Ref. 49), and Ellis & Werner (Ref. 28) have subsequently published fluxes from NGC 7027 for both this line and for [O I] 146μm and [C II] 158μm. They attributed the lines to emission from a circumnebular photodissociation zone having an atomic hydrogen density of $5 \times 10^4 \text{ cm}^{-3}$ and a temperature of 300K, with a mass of 0.3 M_{\odot} . Dinerstein *et al.* (Ref. 24) have detected [O I] 63μm emission from three other dense PN, at a level ten times lower than that from NGC 7027. Future *KAO* and *ISO* observations of these lines hold great promise as a tool for determining the physical parameters of the atomic and molecular neutral zones around optically thick PN, since these zones are very hard to study by non-IR techniques.

3. MOLECULAR HYDROGEN

Black (Ref. 10) has reviewed PN molecular hydrogen observations and theory for the period up to 1982. Since then, three significant surveys of molecular hydrogen emission from planetary nebulae have been published (Refs. 42, 71, 77). These surveys principally consisted of low-resolution CVF spectroscopy around the wavelength of the $v=1-0$ S(1) line at $2.12\mu\text{m}$. Webster *et al.* (Ref. 77) have compiled the results of all molecular hydrogen searches, showing that 29 out of the 55 PN so far surveyed have exhibited molecular hydrogen emission, of which 17 have been spatially mapped. One surprising aspect is that, in general, young, dense, optically thick PN, such as IC 418, NGC 6572 and IC 4997, have *not* been detected in H_2 , while a large number of old, low-density PN *have* been detected. This may partly be due to the stronger IR continua of the dense PN reducing the contrast of H_2 lines, so that higher resolving powers would be needed to yield detections (Ref. 25). However, it could be due to a real lack of H_2 in the circumnebular neutral zones around some young optically thick PN, since their relatively cool (for PN) central stars have strong near-UV continua capable of efficiently photodissociating H_2 . For example, IC 418, which is not detected in H_2 (Ref. 71) *has* been detected in atomic hydrogen (Ref. 73) and a H I mass of $0.35 M_\odot$ has been derived.

Another surprising aspect of the molecular hydrogen statistics for PN has been the rather high detection rate of large, evolved PN. Webster *et al.* (Ref. 77) showed that 19 out of the 29 PN so far detected in H_2 could be classified as Type I. These are nebulae, often bipolar, which show greatly enhanced helium and nitrogen abundances (Ref. 57). Examples include NGC 6853 and NGC 7293. They are thought to originate from more massive than average progenitor stars. Their central stars would then have had a short, high-luminosity phase, before declining rapidly to their current, hot, low-luminosity state. It has usually been assumed that the molecular hydrogen detected around these objects must have survived from the cool red giant phase inside neutral optically thick regions. However, the fact that the central stars must once have had much higher ionising luminosities may also imply that material in the outer nebular regions which was once ionised has now recombined. Unfortunately, currently known formation mechanisms do not appear to be able to produce enough H_2 on the required timescales in such recombination zones (Ref. 80).

Models which do not invoke pre-existing H_2 have usually looked to Associative detachment reactions for the formation of H_2 in the ionisation transition zones around optically thick PN (Refs. 9, 11). In these thin regions there will exist significant abundances of hydrogen atoms, protons and electrons, which can enable H_2 to form via the reactions



The reaction rate for (1) is $7 \times 10^{-19} T \text{ cm}^{-3} \text{ s}^{-1}$, while that for (2) is $10^{-9} \text{ cm}^{-3} \text{ s}^{-1}$, so reaction (1) determines the timescale for H_2 formation. For an ionisation transition zone with $T = 1000\text{K}$, this timescale will be $5 \times 10^7 / n_e$ years. NGC 7027 is one of the densest known PN and the electron density in the transition zone, n_e , is thought to be of the order of 10^5 cm^{-3} , so the mechanism may be viable. Because of the narrowness of ionisation transition regions, a very narrow ($\delta R/R = 2 \times 10^{-3}$) H_2 emission zone is predicted. However, spatial mapping (Ref. 8) and imaging (Ref. 70) of NGC 7027 in the $\text{H}_2 v = 2-1$ S(1) and H I B γ lines appears to show that the H_2 emission is much more extended than this.

Three excitation mechanisms for the observed H_2 vibration-rotation emission from PN have been proposed. These are : (A) Direct population of the upper energy levels during the formation of H_2 : detailed modelling (Ref. 11) has shown that this mechanism is insufficient to produce the observed line fluxes. (B) UV-pumped fluorescence (Refs. 9, 11, 12) : in this mechanism high vibrational levels are populated as a result of cascades following the absorption of UV photons by H_2 electronic transitions. (C) Thermal excitation by collisions, for example in shocks (Ref. 69).

UV-pumped fluorescence is not thought to be the principal excitation mechanism in most PN, because it predicts much stronger high vibrational lines than are normally observed. The strength of the $V = 2-1$ S(1) line at $2.25\mu\text{m}$ is predicted to be about one half of that of the $v = 1-0$ S(1) line at $2.12\mu\text{m}$, whereas the observed ratio is almost always much smaller than this (1/16 in NGC 7027, Refs. 8, 72). However, it has recently been found (Ref. 25) that in one PN at least, Hb 12, the observed H_2 relative line fluxes *are* in good agreement with UV-pumped fluorescence model predictions (Ref. 12). This PN is a young, dense, optically thick object and it was found necessary to offset from the bright core in order to detect the fluorescent H_2 emission (Ref. 25).

Collisional excitation of H_2 in a warm gas is thought to be the main mechanism producing the observed $v=1-0$ line fluxes from PN. Smith *et al.* (Ref. 69) derived a rotational excitation temperature of 1100K from the $v=1-0$ lines emitted by NGC 7027, and Isaacman (Ref. 42) derived similar $v=1-0$ rotational excitation temperatures for a number of other PN. Recently, Tanaka *et al.* (Ref. 72) have shown that the $v=2-1/v=1-0$ vibrational temperature for NGC 7027 is significantly larger, at 1900K , and that this may be understood as being due to the $v=2-1$, and higher, transitions being populated by UV fluorescence, while the $v=1-0$ transitions are produced overwhelmingly by collisional excitation from the ground state.

In the ionisation transition zone model of Black *et al.* (Ref. 11) the H_2 emission from NGC 7027 is excited by warm (1000-5000K) gas in the thin ionisation transition zone. Most authors have, however, invoked shock excitation of pre-existing H_2 in the neutral zones around optically thick nebulae, these shocks being precursors of ionisation fronts. For NGC 7027 the ionised gas expansion velocity is 21 km s^{-1} (Ref. 78), while the expansion velocity of the cool extended CO $J=1-0$ emission region surrounding it is $16-18 \text{ km s}^{-1}$ (Refs. 74, 45). The difference between the ionised and neutral region expansion velocities seems insufficient for shock excitation to account for the observed H_2 emission. Recent 12 km s^{-1} resolution spectra of the $H_2 \nu=1-0 S(1)$ line at the centre of NGC 7027 (Refs. 30, 70) reveal the profile to have two peaks, separated by 35 km s^{-1} . This is consistent with emission from a hollow shell (the interior being filled by ionised gas) with the separation of the peaks being equal to twice the expansion velocity of the shell. The resulting expansion velocity is the same as that of the cool CO molecular cloud, so emission of the H_2 in the ionisation transition zone appears to be ruled out, as does shock excitation. Photodissociation zone models would seem relevant here and it would be of interest to see such models calculated for PN parameters, since Hollenbach (Ref. 41) has pointed out that at high densities the lower vibrational levels of H_2 should be thermalised at 1000-3000K by collisions in the photodissociation region.

4. DUST EMISSION FEATURES

Planetary nebulae have proved to be of great importance for determining the nature of the materials responsible for the various infrared dust features. This is because (a) their nebular C/O ratios show a much larger range than is found in interstellar environments and (b) these C/O ratios can be accurately derived. I have reviewed the observations of dust emission features from PN for the period up to 1983 (Ref. 6), while Roche (Refs. 62, 63) has reviewed subsequent work. The work of Aitken & Roche (*e.g.* Ref. 2) had built up a sufficient sample for them to show that those PN exhibiting the $9.7\mu\text{m}$ silicate feature had C/O ratios less than unity (as determined from UV/optical nebular analyses), while those PN exhibiting strongly the $11.2\mu\text{m}$ SiC feature had C/O ratios larger than unity. This was in agreement with expectations that silicate and SiC grains respectively required oxygen-rich and carbon-rich environments for their formation. The silicate-feature PN had a mean C/O ratio of 0.4 (consistent with the solar ratio), while three SiC-feature PN were found to have C/O ratios ranging from 0.9 to 1.3, consistent with C/O ratios larger than unity once the small contribution from C locked up in SiC is allowed for.

A significant number of PN exhibit the family of unidentified infrared (UIR) bands which are discussed extensively elsewhere in these Proceedings, and I have shown (Ref. 6) that those PN whose spectra are dominated by the UIR bands have even larger C/O ratios (≥ 2) than do the PN whose $10\mu\text{m}$ spectra are dominated by the SiC feature. This strongly supported the identification of the UIR bands with grain-associated hydrocarbons. Cohen *et al.* (Refs. 20, 22) have shown that there is a very good correlation between the nebular C/O ratio and $f(7.7)$, the fraction of the total IR luminosity emitted in the $7.7\mu\text{m}$ UIR band. Their $4-8\mu\text{m}$ data showed that the UIR bands are in fact present, although more weakly, in the spectra of PN with strong SiC features. It appears that the SiC and UIR bands can occur in all PN with $C/O \geq 1$, with SiC dominating at low C/O ratios and the UIR bands dominating at higher C/O ratios. Current statistics, as summarised by Roche (Ref. 62) show that of those PN with detectable $10\mu\text{m}$ continua, 33% show the $9.7\mu\text{m}$ silicate feature, 25% show the $11.5\mu\text{m}$ SiC feature strongly and 42% show the UIR bands strongly (the remainder have continua which are too weak to classify).

High spectral resolution observations of the UIR bands have mainly concentrated on the $3.3\mu\text{m}$ feature. Geballe *et al.* (Ref. 31), using a resolving power of $R=400$, found that NGC 7027 and BD+30°3639 both showed, in addition to the strong $3.3\mu\text{m}$ feature, the weaker $3.4\mu\text{m}$ feature plus a broad plateau of emission centred around $3.45\mu\text{m}$. Observations made at $R=1500$ have since shown (Ref. 55) that this 'plateau' consists of features at $3.46\mu\text{m}$ and $3.52\mu\text{m}$, and possibly at $3.55\mu\text{m}$ and $3.58\mu\text{m}$. These observations also showed that the $3.3\mu\text{m}$ features emitted by NGC 7027 and the PN IRAS 21282+5050 had virtually identical profiles, while Takanaga *et al.* (Ref. 75) have found that the $3.3\mu\text{m}$ feature of HD 44179 (a probable proto-PN) is significantly narrower than that of NGC 7027.

Spatially resolved IR spectroscopy of PN has proved useful for constraining the excitation mechanisms of the UIR bands. Aitken & Roche (Ref. 3) obtained spatial scans of NGC 7027 at 30 different wavelengths between $10\mu\text{m}$ and $13\mu\text{m}$ which showed that the $11.3\mu\text{m}$ UIR band peaked 1.5 arcsec outside both the ionised gas and dust continuum emission peaks – the material emitting the band must therefore largely lie outside the ionised zone, in the neutral shell. Infrared camera images of NGC 7027 at the wavelength of the $3.3\mu\text{m}$ band show the same behaviour (Ref. 63).

Forrest *et al.* (Ref. 29) discovered a strong, broad dust emission feature, extending from $24\mu\text{m}$ to at least $30\mu\text{m}$, in the spectra of several carbon stars and PN with strong SiC features (the IR energy distribution of one of these PN, IC 418, is illustrated in Figure 1). Subsequent observations have shown the feature to peak at about $35\mu\text{m}$ and to extend from approximately $24-44\mu\text{m}$

(Refs. 33, 53, 32). An identification of the feature with MgS has been proposed (Ref. 32) and laboratory spectra of this material do indeed provide a very good fit to the observations (Ref. 56). However, in the case of IC 418 almost 25% of the total IR luminosity is emitted in this feature (Ref. 53 and Figure 1). This seems a surprisingly high fraction for a material limited by the abundance of sulphur and magnesium, although Moseley and Silverberg (Ref. 53) have argued that it could be done if the MgS was in the form of a thin layer deposited on SiC grains. Middlemass (Ref. 52) has found magnesium to be undepleted in the nebular gas phase in IC 418. Baron *et al.* (Ref. 5) have suggested that the $35\mu\text{m}$ feature might be due to structure in the absorption efficiency spectrum of graphite, though to date no laboratory graphite or amorphous carbon samples have shown structure having the required amplitude.

5. DUST CONTINUUM EMISSION

At first sight the study of the dust continuum emission from PN might not seem to require spectroscopy. In practice, however, ionic emission lines and dust features are so prevalent that broad-band photometry is frequently seriously affected. This is known to be the case at wavelengths shorter than $20\mu\text{m}$ at which the hottest grains emit. Spectroscopy is therefore usually necessary in order to define the true dust continuum level. A PN's IR continuum flux distribution normally peaks between $25\mu\text{m}$ and $60\mu\text{m}$, nicely bracketted by the four *IRAS* filter bandpasses. It is fairly straightforward to correct the *IRAS* photometric fluxes for fine structure line emission, if complementary optical spectra of the nebula are available, enabling the IR line fluxes to be predicted. However, unsuspected dust emission features may be lurking within the longer wavelength *IRAS* bandpasses. For instance, we do not know how many PN have their $25\mu\text{m}$ fluxes inflated to some degree by the broad $35\mu\text{m}$ feature (Figure 1). Low-resolution *ISO* spectra of a significant sample of PN are desirable, in order to resolve these questions.

The modelling of grain emission from planetary nebulae has progressed significantly in recent years. In 1981 Natta & Panagia (Ref. 55) carried out a differential analysis of the then available far-infrared data for ten PN. Assuming that the emitting dust resided only within the ionised zone, they found that the gas-to-dust mass ratio increased significantly with increasing nebular radius, appearing to imply that the dust was being destroyed as the nebulae evolved. Since then, major advances have occurred in both the quantity of far-infrared data available and in the dust modelling techniques used to model them. Nearly one thousand PN are listed in the *IRAS* Point Source Catalog (see Ref. 61), and sixty-seven of them

have *IRAS* pointed observations available (Ref. 47). On the theoretical front, nebular ionisation structure codes have been enhanced so as to treat self-consistently the emission by dust grains with various compositions (with realistic size distributions and experimentally determined optical constants) immersed in direct stellar and diffuse nebular radiation fields. A review of these developments has been given by Harrington (Ref. 34).

The first application of such a code to fitting the dust emission from a PN (IC 3568, Ref. 21) adopted carbon smoke grains with a single radius ($0.015\mu\text{m}$). A gas-to-dust mass ratio of 1300 was derived. Harrington *et al.* (Ref. 35) have modelled the dust emission from NGC 3918, using graphite and amorphous carbon grains with MRN size distributions. For both grain types the maximum grain size needed was similar to that of the standard MRN model ($0.25\mu\text{m}$), but their graphite grain model required a lower grain radius cut-off of $0.04\mu\text{m}$ (versus $0.005\mu\text{m}$ for the standard MRN mixture), because smaller grains produced too much flux at $10\mu\text{m}$. Amorphous carbon grains, on the other hand, required a lower grain radius cut-off of $0.0005\mu\text{m}$ in order to produce enough flux at $10\mu\text{m}$. The graphite and amorphous carbon grain models for NGC 3918 yielded gas-to-dust mass ratios of 1300 and 3500, respectively. Harrington *et al.* noted that if the observations had been modelled by blackbody emission corresponding to a single-temperature, single grain size, as has often been the practice, a much lower gas-to-dust mass ratio of 500 would have been derived.

NGC 3918 lies on the borderline between optical thickness and thinness to the hydrogen Lyman continuum. Hoare (Ref. 39) has modelled the dust emission from the lower-density, optically thin nebula NGC 7662 and, using MRN grain size distributions, derived gas-to-dust mass ratios similar to those found for NGC 3918 (Table 3). He also modelled the dust emission from the higher-density, optically thick nebula IC 418, the model incorporating a treatment of the emission from grains residing in the neutral zone. Figure 1 shows Hoare's best-fitting models, which use graphite or amorphous carbon grains, along with silicon carbide grains (available optical constants did not allow a treatment of the $35\mu\text{m}$ MgS feature). At the shortest infrared wavelengths plotted, there is a noticeable broad-band excess relative to the level predicted for the summed stellar, nebular and dust continua. At K and L, mapping observations have shown that this excess largely originates from outside the ionised boundary of IC 418 (Refs. 58, 59).

Table 3 summarises the gas-to-dust mass ratios that have been derived for the three carbon-rich PN that have so far been modelled using the techniques described above. The mean nebular densities span a range of a factor of three but the derived gas-to-dust ratios differ by no more than a factor of two. As the sample increases in size, it should become clear whether PN gas-to-dust ratios do in

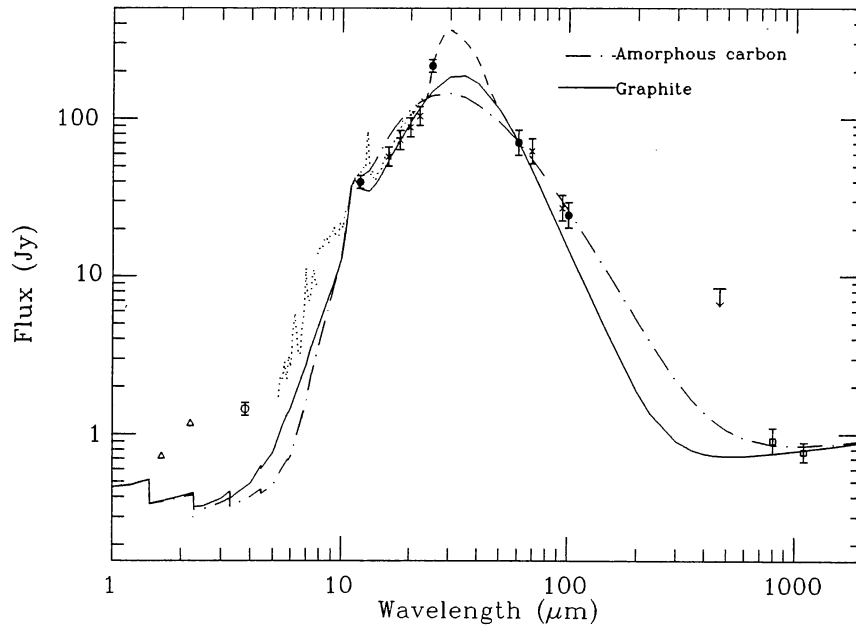


Figure 1. The infrared flux distribution of IC 418 and the best-fitting amorphous carbon and graphite grain models (Ref. 40)

Table 3. Gas-to-dust mass ratios for three carbon-rich planetary nebulae

NAME	C/O	n_e (cm^{-3})	$M_{\text{gas}}/M_{\text{dust}}$		Ref.
			Graphite	Amorphous carbon	
IC 418	1.3	9000	1100	1800	40
NGC 3918	1.6	6000	1300	3500	35
NGC 7662	1.7	2500	2300	3500	40

fact change significantly as the nebulae evolve. The gas-to-dust mass ratios listed for the the three PN in Table 3 are factors of five to ten times smaller than those usually estimated for the interstellar medium. If the respective ratios estimated for the ISM and for PN are correct, the implication must be that PN cannot contribute significantly to the interstellar dust content, a rather surprising result in view of the fact that the red giant progenitors of PN are thought to be the major source of refractory interstellar grains. It will also be of interest to see what gas-to-dust mass ratios are needed for silicate grain models of oxygen-rich PN. The only such work published to date (Ref. 40) was for the halo PN DDDM-1, for which a gas-to-dust mass ratio of 900 was derived.

For all four of the PN with detailed dust models, discussed above, Ly- α photons provide about 55% of the grain heating, with the balance provided by the direct absorption of stellar continuum photons, apart from NGC 3918, for which CIV and NV resonance line photons provide 17% of the heating. In no case was dust found to compete significantly for ionising photons or to affect the nebular ionisation structure.

6. REFERENCES

1. Aggarwal, K. M., 1983, *J. Phys. B*, **16**, 2405.
2. Aitken, D. K. & Roche, P.F., 1982, *Mon. Not. R. astr. Soc.*, **200**, 217.
3. Aitken, D. K. & Roche, P.F., 1983, *Mon. Not. R. astr. Soc.*, **202**, 1233.
4. Ashley, M. C. B. & Hyland, A. R., 1988, *Astrophys. J.*, **331**, 532.
5. Baron, Y., de Muizon, M., Papoular, R. & Pegourie, B., 1987, *Astr. Astrophys.*, **186**, 279.
6. Barlow, M. J., 1983, *Proc. IAU Symp. No. 103*, ed. D. R. Flower, Reidel, Dordrecht, Holland, 105-127.
7. Bayes, F. A., Saraph, H. E. & Seaton, M. J., 1985, *Mon. Not. R. astr. Soc.*, **215**, 85P.
8. Beckwith, S., Neugebauer, G., Becklin, E. E. & Matthews, K., 1980, *Astr. J.*, **85**, 886.
9. Black, J. H., 1978, *Astrophys. J.*, **222**, 125.
10. Black, J. H., 1983, *Proc. IAU Symp. No. 103*, ed. D. R. Flower, Reidel, Dordrecht, Holland, 91-100.
11. Black, J. H., Porter, A. & Dalgarno, A. 1981, *Astrophys. J.*, **249**, 138.
12. Black, J. H. & van Dishoeck, E. F. 1987, *Astrophys. J.*, **322**, 412.
13. Bohlin, R. C., Marionni, P. A., Stecher, T. P., 1975, *Astrophys. J.*, **202**, 415.
14. Bregman, J. D., Dinerstein, H. L., Goebel, J. H., Lester, D. F., Witteborn, F. C. & Rank, D. M., 1983, *Astrophys. J.*, **274**, 666.
15. Butler, K., 1989, *In preparation*.
16. Butler, K. & Mendoza, C., 1984, *Mon. Not. R. astr. Soc.*, **208**, 17P.
17. Butler, K. & Storey, P. J., 1989, *In preparation*.
18. Clegg, R. E. S., 1989, *Proc. IAU Symp. No. 131*, ed. S. Torres-Peimbert, Reidel, Dordrecht, Holland, 139-156.
19. Clegg, R. E. S., Harrington, J. P., Barlow, M. J. & Walsh, J. R., 1987, *Astrophys. J.*, **314**, 551.
20. Cohen, M., Allamandola, L., Tielens, A.G.G.M., Bregman, J., Simpson, J.P., Witteborn, F. C., Wooden, D. & Rank, D., 1986, *Astrophys. J.*, **302**, 737.
21. Cohen, M., Harrington, J. P. & Hess, R., 1984, *Astrophys. J.*, **283**, 687.
22. Cohen, M., Tielens, A.G.G.M., Bregman, J., Witteborn, F. C., Rank, D., Allamandola, L. J., Wooden, D. H. & de Muizon, M., 1989 *Astrophys. J.*, In Press.
23. Dinerstein, H. L., 1983, *Proc. IAU Symp. No. 103*, ed. D. R. Flower, Reidel, Dordrecht, Holland, 79-88.
24. Dinerstein, H. L., Ellis, H. B., Haas, M. R. & Werner, M. W., 1985, *B.A.A.S.*, **17**, 908.
25. Dinerstein, H. L., Lester, D. F., Carr, J. S. & Harvey, P. M., 1988, *Astrophys. J.*, **327**, L27.
26. Dinerstein, H. L., Lester, D. F. & Werner, M. W., 1985, *Astrophys. J.*, **291**, 561.
27. Dinerstein, H. L. & Werner, M. W., 1989, *Proc. IAU Symp. No. 131*, ed. S. Torres-Peimbert, Reidel, Dordrecht, Holland, 214.
28. Ellis, H. B. & Werner, M. W., 1984, *B.A.A.S.*, **16**, 463.
29. Forrest, W.J., Houck, J. R. & McCarthy, J. F., 1981, *Astrophys. J.*, **248**, 195.
30. Geballe, T. R., 1988, *Molecular Astrophysics*, ed. T. W. Hartquist, Cambridge Univ. Press, Cambridge, England, In Press.
31. Geballe, T. R., Lacy, J. H., Persson, S. E., McGregor, P. J. & Soifer, B. T., 1985, *Astrophys. J.*, **292**, 500.
32. Glaccum, W. J., 1989, *These Proceedings*.
33. Goebel, J. H. & Moseley, S. H., 1985, *Astrophys. J.*, **290**, L35.
34. Harrington, J. P., 1987, *Proc. Vulcano Workshop 'Planetary and Protoplanetary Nebulae, from IRAS to ISO'* ed. A. Preite-Martinez, Reidel, Dordrecht, Holland, 239-245.
35. Harrington, J. P., Monk, D. J. & Clegg, R. E. S., 1988, *Mon. Not. R. astr. Soc.*, **231**, 571.
36. Harrington, J. R., Seaton, M. J., Adams, S. & Lutz, J. H., 1982, *Mon. Not. R. astr. Soc.*, **199**, 577.
37. Hayes, M. A. & Nussbaumer, H., 1983, *Astr. Astrophys.*, **124**, 279.
38. Hayes, M. A. & Nussbaumer, H., 1984, *Astr. Astrophys.*, **134**, 193.
39. Hoare, M. G., 1988, *Ph.D. Thesis*, Univ. of London.

40. Hoare, M. G. & Clegg, R. E. S., 1988, *Mon. Not. R. astr. Soc.*, **235**, 1049.
41. Hollenbach, D., 1988, *Astrophys. Letters*, **26**, 191.
42. Isaacman, R., 1984, *Astr. Astrophys.*, **130**, 151.
43. Johnson, C. T., Kingston, A. E. & Dufton, P. L., 1986, *Mon. Not. R. astr. Soc.*, **220**, 155.
44. Keenan, F. P., Lennon, D. J., Johnson, C. T. & Kingston, A. E., 1986, *Mon. Not. R. astr. Soc.*, **220**, 571.
45. Knapp, G. R. & Morris, M., 1985, *Astrophys. J.*, **292**, 640.
46. Lambert, D. L., Gustafsson, B., Eriksson, K. & Hinkle, K. H., 1986, *Astrophys. J. Suppl.*, **62**, 373.
47. Leene, A. & Pottasch, S. R., 1988, *Astr. Astrophys.*, **202**, 203.
48. Lennon, D. J., Dufton, P. L., Hibbert, A. & Kingston, A. E., 1985, *Astrophys. J.*, **294**, 200.
49. Melnick, G., Russell, R. W., Gull, G. E. & Harwit, M., 1981, *Astrophys. J.*, **243**, 170.
50. Mendoza, C., 1983, *Proc. IAU Symp. No. 103*, ed. D. R. Flower, Reidel, Dordrecht, Holland, 143-172.
51. Mendoza, C. & Zeppen, C. J., 1987, *Mon. Not. R. astr. Soc.*, **224**, 7P.
52. Middlemass, D., 1988, *Mon. Not. R. astr. Soc.*, **231**, 1025.
53. Moseley, S. H. & Silverberg, R. F., 1986, *Interrelationships among Circumstellar, Interstellar and Interplanetary Dust*, ed. J. A. Nuth & R. E. Stencel, NASA CP-2403, A18.
54. Nagata, T., Tokunaga, A. T., Sellgren, K., Smith, R. G., Onaka, T., Nakada, Y. & Sakata, A., 1988, *Astrophys. J.*, **326**, 157.
55. Natta, A. & Panagia, N., 1981, *Astrophys. J.*, **248**, 189.
56. Nuth, J. A., Moseley, S. H., Silverberg, R. F., Goebel, J. H. & Moore, J. W. 1985, *Astrophys. J.*, **290**, L41.
57. Peimbert, M. & Torres-Peimbert, S., 1983, *Proc. IAU Symp. No. 103*, ed. D. R. Flower, Reidel, Dordrecht, Holland, 233-241.
58. Phillips, J. P., Sanchez Magro, F. & Martinez Roger, C., 1984, *Astr. Astrophys.*, **133**, 395.
59. Phillips, J. P., Mampaso, A., Vilchez, J. M. & Gomez, P., 1986, *Astrophys. Sp. Sci.*, **122**, 81.
60. Pottasch, S. R., Preite-Martinez, A., Olton, F. M., Mo Jing-Er, Kingma, S., 1986, *Astr. Astrophys.*, **161**, 363.
61. Preite-Martinez, A., 1989, *Proc. IAU Symp. No. 131*, ed. S. Torres-Peimbert, Reidel, Dordrecht, Holland, 9-16.
62. Roche, P. F., 1987, *Proc. Vulcano Workshop 'Planetary and Protoplanetary Nebulae, from IRAS to ISO'* ed. A. Preite-Martinez, Reidel, Dordrecht, Holland, 45-52.
63. Roche, P. F., 1989, *Proc. IAU Symp. No. 131*, ed. S. Torres-Peimbert, Reidel, Dordrecht, Holland, 117-127.
64. Roche, P. F. & Aitken, D. K., 1983, *Mon. Not. R. astr. Soc.*, **203**, 9P.
65. Roche, P. F. & Aitken, D. K., 1986, *Mon. Not. R. astr. Soc.*, **221**, 63.
66. Rowlands, N., Houck, J. R., Herter, T., Gull, G. E. & Skrutskie, M. F., 1989, *Astrophys. J.*, In Press.
67. Shure, M. A., Herter, T. & Houck, J. R., 1983, *Astrophys. J.*, **274**, 646.
68. Shure, M. A., Houck, J. R., Gull, G. E. & Herter, T., 1984, *Astrophys. J.*, **281**, L29.
69. Smith, H. A., Larson, H. P. & Fink, U., 1981, *Astrophys. J.*, **244**, 835.
70. Smith, M. G., Geballe, T. R., Aspin, C. A., McLean, I. S. & Roche, P. F., 1989, *Proc. IAU Symp. No. 131*, ed. S. Torres-Peimbert, Dordrecht, Reidel, Holland, 178.
71. Storey, J. W. V., 1984, *Mon. Not. R. astr. Soc.*, **206**, 521.
72. Tanaka, M., Hasegawa, T., Hayashi, S. S., Brand. P. W. J. L. & Gatley, I., 1989, *Astrophys. J.*, **336**, 207.
73. Taylor, A. R., Gussie, G. T. & Goss, W. M., 1989, *Astrophys. J.*, In Press.
74. Thronson, H. A., 1983, *Astrophys. J.*, **264**, 599.
75. Tokunga, A. T., Nagata, T., Sellgren, K., Smith, R. G., Onaka, T., Nakada, Y., Sakata, A. & Wada, S., 1988, *Astrophys. J.*, **328**, 709.
76. Watson, D. M., 1983, *Proc. XVIth ESLAB Symposium*, ed. M. F. Kessler & J. P. Phillips, Reidel, Dordrecht, Holland, 193-217.
77. Webster, B. L., Payne, P. W., Storey, J. W. V. & Dopita, M. A., 1988, *Mon. Not. R. astr. Soc.*, **235**, 533.
78. Wilson, O. C., 1950, *Astrophys. J.*, **111**, 279.
79. Zeppen, C. J., Butler, K. & Le Boulrot, J., 1987, *Astr. Astrophys.*, **188**, 251.
80. Zuckerman, B. & Gatley, I., 1988, *Astrophys. J.*, **324**, 501.